Received: 15 August 2021 | Revised: 23 October 2021 | Accepted: 27 October 2021

DOI: 10.1002/jcb.30174

RESEARCH ARTICLE

Journal of Cellular Biochemistry WILEY

Understanding the binding mechanism for potential inhibition of SARS-CoV-2 Mpro and exploring the modes of ACE2 inhibition by hydroxychloroquine

Manisha Choudhury[1] | **Anantha K. Dhanabalan**[2] | **Nabajyoti Goswami**[3]

[1]Department of Biosciences and Bioengineering, IIT Bombay, Mumbai, Maharashtra, India

[2]CAS in Crystallography and Biophysics, University of Madras, Chennai, Tamil Nadu, India

[3]Bioinformatics Infrastructure Facility, College of Veterinary Science, Assam Agricultural University, Khanapara, Guwahati, Assam, India

Correspondence
Manisha Choudhury, Department of Biosciences and Bioengineering, IIT Bombay, Powai, Mumbai 400076, India.
Email: choudhurymanisha.00@gmail.com

Abstract

As per the World Health Organization report, around 226 844 344 confirmed positive cases and 4 666 334 deaths are reported till September 17, 2021 due to the recent viral outbreak. A novel coronavirus (severe acute respiratory syndrome coronavirus 2 [SARS-CoV-2]) is responsible for the associated coronavirus disease (COVID-19), which causes serious or even fatal respiratory tract infection and yet no approved therapeutics or effective treatment is currently available to combat the outbreak. Due to the emergency, the drug repurposing approach is being explored for COVID-19. In this study, we attempt to understand the potential mechanism and also the effect of the approved antiviral drugs against the SARS-CoV-2 main protease (Mpro). To understand the mechanism of inhibition of the malaria drug hydroxychloroquine (HCQ) against SARS-CoV-2, we performed molecular interaction studies. The studies revealed that HCQ docked at the active site of the Human ACE2 receptor as a possible way of inhibition. Our in silico analysis revealed that the three drugs Lopinavir, Ritonavir, and Remdesivir showed interaction with the active site residues of Mpro. During molecular dynamics simulation, based on the binding free energy contributions, Lopinavir showed better results than Ritonavir and Remdesivir.

KEYWORDS

ACE-2, hydroxychloroquine, Lopinavir, Mpro, Ritonavir, SARS-CoV-2

1 | INTRODUCTION

In late December 2019, a novel coronavirus that has been formally named severe acute respiratory syndrome coronavirus 2 (SARS-CoV-2) was identified to be the cause of atypical pneumonia outbreak in Wuhan, China, named coronavirus disease 2019 (COVID-19).[1] Since the middle of February 2020, it has spread rapidly throughout the globe with a high mortality rate, and on March 11, 2020, the WHO declared it as a pandemic.

The drug repurposing approach has indeed gained wide attention for the ability to reuse already available drugs for various diseases which were originally developed for specific diseases. Drug repurposing can serve as a short-term and nonspecific solution to treat COVID-19 patients,[2] as reports have shown drugs with multiple protein targets and also many diseases sharing overlapping molecular pathways.[3] Drugs such as Lopinavir (LPN), Nelfinavir, Oseltamivir, Atazanavir, and Ritonavir (RTN) are used to cure Middle East Respiratory syndrome and SARS.[4,5] Reports have shown that Favipiravir,

an approved influenza virus drug, and Sofosbuvir, a hepatitis C virus drug have potential against Ebola and Zika viruses.[6] Several combinations of drugs are also being tested to combat the disease. Recently, a combination of three different drugs, LPN and RTN developed for HIV and Oseltamivir developed for influenza virus has shown potent inhibition against SARS-CoV-2 Mpro in computational studies.[7] Molecular docking and molecular dynamics (MD) simulations studies have been carried out with *Camellia sinensis L* bioactive molecules and FDA drug molecules (Atazanavir, Darunavir, and LPN) against the Mpro of SARS-CoV-2.[8] Similarly, drug repurposing approach studies were employed with FDA-approved drug molecules of anti-HIV (Atazanavir, Indinavir, and Saquinavir) and anti-HCV (Ciluprevir and Glecaprevir) with main protease Mpro of SARS-CoV-2.[9] Recently, inhibition of several drug targets proteins of SARS-CoV-2 (RNA-dependent RNA polymerase, nonstructural protein 16, nonstructural protein-15, Spike protein ACE2, and nonstructural protein 1) have been carried out with computational approaches to understand the binding mechanism of the identified lead compounds.[10–14]

Research efforts to develop antiviral agents against the Coronaviridae family have shown that the angiotensin-converting enzyme II (ACE2) entry receptor, the RNA-dependent RNA polymerase (RdRp) and the main protease (Mpro) proteins represent drug targets.[15] Due to significant side effects, initially promising inhibitors of ACE2 did not advance clinically.[16] However, what has drawn maximum attention are the recent reports on using hydroxychloroquine (HCQ) as prophylaxis to prevent COVID-19 infections. A study on the inhibitor effect of Remdesivir (RMD) (an antiviral drug) and Chloroquine (an old antimalarial drug) on the growth of SARS-CoV-2 in vitro is recently reported.[2] Savarin et al.[17] reported that chloroquine showed inhibition of SARS-CoV entry by changing the glycosylation of ACE2 receptor and spike protein.[17] Studies have also shown that HCQ treatment significantly decreased the viral load in COVID-19 patients.[18,19] There are no conclusive scientific reports on the mechanism of inhibition by HCQ in COVID-19 infections and therefore, we attempt to study the possible binding mode of HCQ to ACE2 receptor preventing binding of spike protein and thus, SARS-CoV-2 entry into the host. The nonstructural proteins (nsps) generated by SARS-CoV-2 Mpro play a major role in viral replication.[20] Mpro is a homodimer that comprises three structural domains, Domain I, II, and III.[21] The substrate-binding site is located at the Cys-His catalytic dyad in a cleft between Domain I and II.[22]

Due to the significant role of Mpro in self maturation and subsequent maturation of polyproteins, it has emerged as a significant antiviral target in COVID-19. In this study, we attempt to understand the binding mechanism for potential inhibition of SARS-CoV-2 Mpro and investigate the mode of ACE2 inhibition by Hydroxychloroquine.

2 | MATERIALS AND METHODS

2.1 | Data set preparation

Drugs with antiviral properties such as RTN, Zanamivir, Peramivir, RMD, Ribavirin, Oseltamivir, LPN Baloxavir, Dasabuvir, Favipiravir, Ombitasvir, and Paritaprevir were screened against the target protein SARS-CoV-2 Mpro. Furthermore, hydroxychloroquine was screened against the target protein Human ACE2 receptor. All the listed approved drugs considered in the study were retrieved from the PubChem database. All the compounds were built using a builder panel in Maestro. The compounds were processed for ligand preparation step using Ligprep 2.3 module (Schrödinger) which performs addition of hydrogen,[23] two-dimensional (2D) to three-dimensional (3D) conversion, realistic bond lengths and bond angles, low energy structure with correct chiralities, ionization states, tautomers, stereo chemistries, and ring conformations. Ionization of all the compounds was optimized using an inbuilt Epik module in Schrödinger.[24]

The target protein SARS-CoV-2 main protease, Human ACE2 receptor were obtained from Protein Data Bank at (http://www.rcsb.org) (PDBID: 5R82, 1R4L). Missing hydrogen atoms were added and correct bond orders were assigned,[25] and then formal charges and orientation of various groups were fixed. Following this, optimization of the amino acid orientation of hydroxyl groups, amide groups was carried out.[26] All amino acid flips were assigned and H-bonds were optimized. No hydrogen atoms were minimized until the average root mean square deviation reached the default value of 0.3 Å.[27]

2.2 | Screening of approved drugs against COVID-19 drug targets

Molecular docking studies were carried out using Schrodinger Glide XP (Extra precision)[28] with default parameters. To facilitate the best possible conformation, a wide range of searches were carried out. The docking grid box size was set to $12 \times 12 \times 12$ Å dimension centered at X, Y, and Z coordinate. Minimization cycle for Conjugate Gradient (CG) and steepest descent minimizations were used with the default value of 0.05 Å for

initial step size and 1.0 Å for the maximum step size. In convergence criteria for the minimization, the energy change criteria and gradient criteria were set at a default value of 10^{-7} and 0.001 kcal/mol, respectively.[29] Following this, all conformations were considered for docking studies. Glide score and Glide energy were used to select the best conformation for each ligand.

2.3 | Free energy calculation (Prime MM/GBSA)

The best drug candidate (RTN, LPN, and RMD) docked complexes were carried forward for binding free energy calculation using a prime module.[30] $E_{complex}$, $E_{protein}$, and E_{ligand} are the minimized energies of the protein–inhibitor complex, protein, and inhibitor, respectively. ΔG solv is generalized born electrostatic solvation energy of the complex. ΔGSA is a nonpolar contribution to the solvation energy due to the surface area. Prime uses a surface generalized born model employing a Gaussian surface instead of a vdW (van der Waal's) surface for better representation of the solvent-accessible surface area[30]

$$\Delta DE = E_{complex} + E_{protein} + E_{ligand}$$

2.4 | Molecular dynamics simulation

All MD simulations were conducted for a time scale of 100 ns each at 310 K (37°C) on a DELL PowerEdge R740 Rack server machine comprising 40 physical processor cores within two second Generation Intel® Xeon®Gold Scalable processors accelerated by an *NVIDIA®-Tesla®V100* Tensor Core graphic processor unit (GPU) using Amber99SB-ILDN force field embedded in GROMACS 2019.5 package.[31–37] Topology files of the drugs LPN, RTN, and RMD were generated by ACPYPE.[38] All systems were prepared in the same way as described here. A water box of 5 Å from the surface of the protein–ligand complex was created for all three systems. All defined protein–ligand systems were solvated with the TIP3P explicit solvent water model. Before energy minimization, four Na+ ions were added to neutralize the systems. The systems were neutralized with counter-ions and energy minimization was performed using the steepest descent method for 50 000 steps. For all three systems, the protein backbone was kept restrained and solvent molecules with counter-ions were subjected to two 500 ps position restrained equilibration MD runs under NVT followed by NPT ensemble with periodic boundary conditions. V-rescale and Berendsen's coupling algorithms were used to keep the temperature (310 K) and pressure (1 bar) constant, respectively. Finally, 100 ns of production MD runs were performed allowing all molecules to move in all directions according to a classical Newtonian leap-frog MD integrator. For all the systems, the pressure was maintained at 1 bar by isotropic pressure coupling in x, y, and z components to a Parrinello–Rahman barostat with a time constant $\tau = 2.0$ ps and compressibility of 4.5×10^{-5} bar^{-1} in all three dimensions. The electrostatic interactions were calculated by the PME algorithm, with a Coulomb cutoff of 12 Å and interpolation order of 4 within a grid spacing of 1.6 Å. The time steps for the simulations were 2 fs and the coordinates were stored every 5 ps. The van der Waals (vdw) forces were treated using a cutoff of 12 Å with force-switch vdw-modifier and rvdw-switch value of 1. LINCS algorithm was used to constrain hydrogen bond lengths as implemented in the used force field. The analyses were performed using GROMACS 2019.5 package and the plots were viewed using GRACE (1991-1995 Paul J Turner, Portland, 1996-2007 Grace Development Team).

2.5 | Binding free energy calculation (MM-PBSA)

Binding free energies (ΔG_{Bind}) of the protein–ligand complexes were calculated from molecular mechanics Poisson–Boltzmann surface area (MM-PBSA) performed by adaptive Poisson–Boltzmann solver 3.0 (APBS 3.0) using g_mmpbsa package.[39,40] The MM-PBSA approach is of the most widely used methods to compute interaction energies among the biomolecular complexes. Together with MD simulation, MM-PBSA can decode significant conformational fluctuations and entropic contributions to the binding energy.[41] In general, the binding free energy between a protein and a ligand in solvent can be expressed as:

$$\Delta DG_{Bind} = G_{Complex} - (G_{Protein} + G_{ligand}),$$

where, $G_{Complex}$ is the total free energy of the protein−ligand complex and $G_{Protein}$ and G_{Ligand} are total free energies of the separated protein and ligand in solvent, respectively.

3 | RESULTS AND DISCUSSION

3.1 | Molecular docking studies with SARS-CoV-2 main protease

There are extensive reports that have investigated the repurposing of antiviral drugs against SARS-CoV-2 Mpro.[42–44] In this study, FDA-approved antiviral compounds were

TABLE 1 Docking results of best FDA-approved antiviral drugs with SARS-CoV-2 main protease

Compounds	Glide gscore (kcal/mol)	Glide energy (kcal/mol)	Hydrogen bond interactions
Ritonavir (RTN)	−10.40	−77.30	Gly143, Asn142, Glu166, Gln189.
Remdesivir (RMD)	−6.97	−55.35	Gln189, Thr26, Gly143, Glu166.
Lopinavir (LPN)	−6.12	−51.77	Thr26, Thr24.
Cocrystal (RZS)	−3.83	−21.33	Arg188.

Abbreviation: SARS-CoV-2, severe acute respiratory syndrome coronavirus 2.

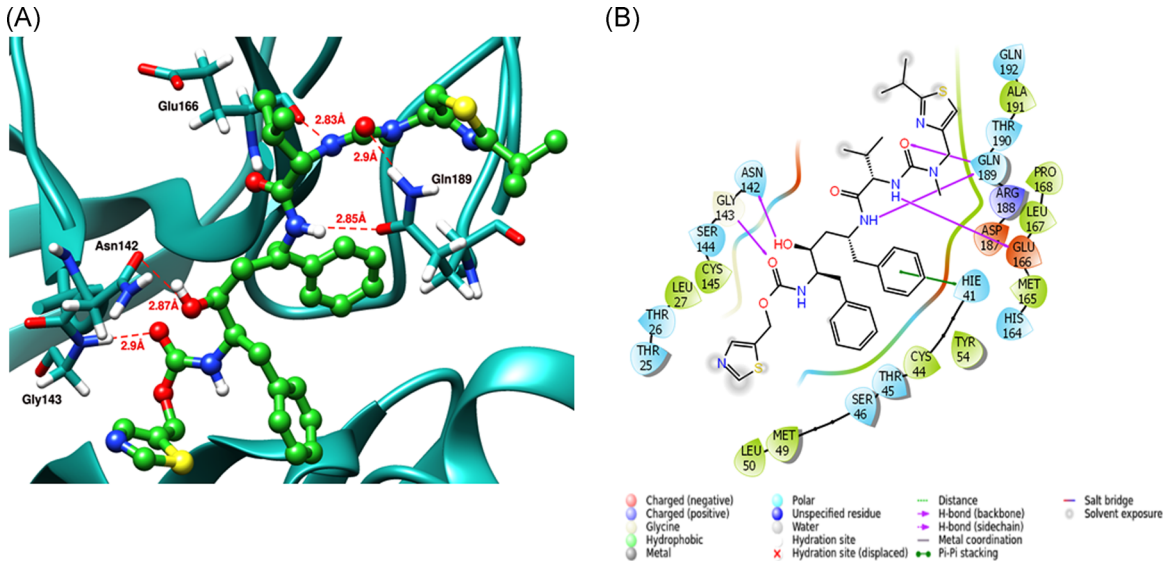

FIGURE 1 Key binding interaction profile of Ritonavir (RTN) docked with SARS-Cov-2 Mpro (A) 3D chimera view (B) 2D maestro view. SARS-CoV-2, severe acute respiratory syndrome coronavirus 2

employed in glide XP docking studies with the SARS-CoV-2 Mpro. Table S1 shows the docking score and glide energy of FDA-approved antiviral drugs on docking with SARS-CoV-2 Mpro (PDBID: 5R82). Among them, three drugs RTN, RMD, and LPN exhibited good docking scores and glide energy and key active site interactions compared to known co-crystal RZS (Table 1).

The RTN drug has four hydrogen bond interactions with active sites residues such as Gly143, Asn142, Glu166, and Gln189 at a distance of 2.90 Å, 2.87 Å, 2.83 Å, and 2.85 Å, respectively. The drug showed hydrophobic interactions at the important sites viz CYS145, LEU27, LEU50, MET49, CYS44, TYR54, MET165, LEU167, PRO168, and ALA191 (Figure 1).

RMD forms three hydrogen bond interactions with Gln189, Thr26, Gly143, and Glu166 active sites of the main protease at a distance of 3.1 Å, 2.5 Å, 3.2 Å, and 2.9 Å, respectively, and also have several hydrophobic interactions such as PRO168, MET49, LEU141, PHE140, LEU27, MET165, and LEU167 (Figure 2). The drug LPN showed three hydrogen bond interactions at the active site residues THR26 and THR24. And also pi-pi interactions were observed with HIS41. The drug showed hydrophobic interactions with residues LEU50, MET49, LEU141, PHE140, MET165, and CYS145, respectively (Figure 2S). In addition, the two reference compounds showed lesser binding affinity (glide score and glide energy) compared to the best-selected drug compounds. Furthermore, the best drug compounds were subjected to prime MMGBSA binding free energy calculations. Table 2 depicts that among the three drugs, RTN has a higher total binding energy ΔG_{bind} −57.434 kcal/mol compared with the other two drugs, RMD and LPN have ΔG binding energy −56.507 and −51.078 kcal/mol.

All three docked complexes were superimposed, and it could be observed that these three drugs bind in a similar orientation of binding pattern with all the sub catalytic sites of the main protease target protein and shows the lesser root mean square deviation (RMSD) among each docked complex (Figure 3). The RMSD

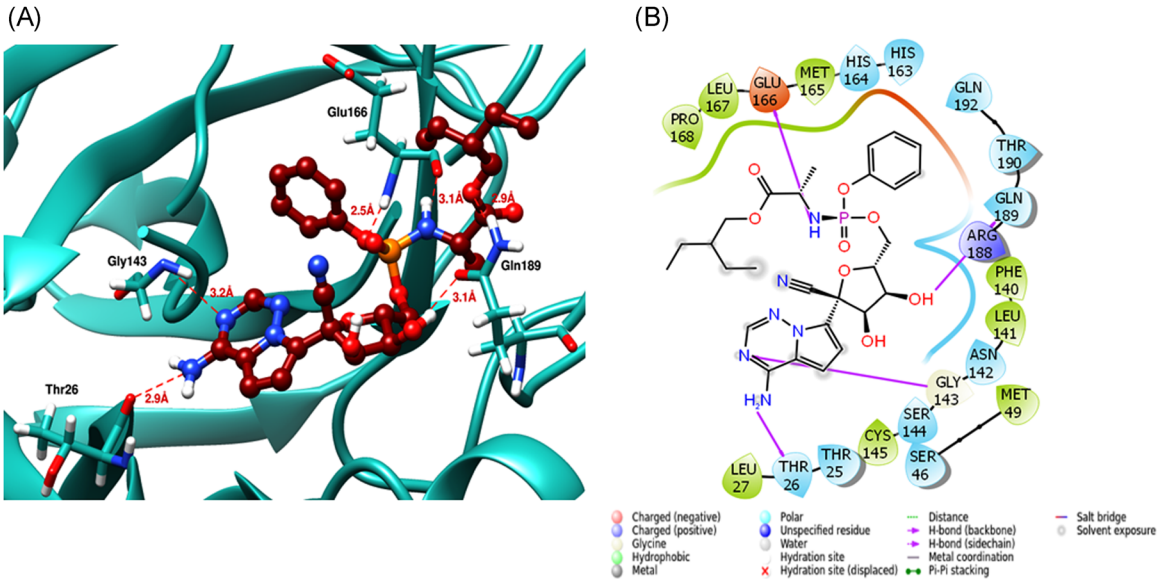

FIGURE 2 Key binding interaction profile of Remdesivir (RMD) docked with SARS-Cov-2 Mpro (A) 3D chimera view (B) 2D maestro view. SARS-CoV-2, severe acute respiratory syndrome coronavirus 2

TABLE 2 Free energy calculation for best-approved drugs Ritonavir (RTN), Remdesivir (RMD), and Lopinavir (LPN)

Compounds	ΔG bind	Coulomb	H-bond	vdW
RTN	−57.434	−21.765	−1.598	−63.968
RMD	−56.507	−28.861	−2.42	−49.35
LPN	−51.078	−17.047	−2.075	−53.17

values of RMD with LPN and RTN is 2.7 Å and 2.3 Å, respectively, and between RTN and LPN is 2.2 Å. From the docking studies, we observed that out of the 12 antiviral drugs considered in this study to inhibit SARS-CoV-2 Mpro, based on the docking score, glide energy, interactions with active site pocket residues and ΔG_{bind}, drugs RTN, RMD, and LPN showed high potential as inhibitors.[7] also reported that LPN and RTN showed potent inhibition against SARS-CoV-2 Mpro in computational studies.

3.2 | Binding studies of HCQ against human ACE2 receptor

The first step of the viral replication cycle, that is, attachment to the surface of respiratory cells, is mediated by the spike (S) viral protein. The S protein uses the ACE-2 receptor for entry into the host and uses sialic acids to link to host cell surface gangliosides. As the prophylaxis mechanism of HCQ is still not clear, we carried out biomolecular interaction studies to gather insight into the possible binding mechanisms with the Human ACE2 receptor.

From Figure 3S, it is observed that HCQ binds with the human ACE2 receptor active sites with a docking score and glide energy of −6.34 and −49.34 kcal/mol, respectively. HCQ forms two hydrogen bond interactions with active site amino acids of ASP367 and ASN277 at distances of 2.65 Å and 2.85 Å, respectively (Figure 4A). In addition, pi–pi interactions are also observed from the active site of HIS345, and ionic interactions were found to be LYS363. Several hydrophobic interactions were also observed from the docked complex of HCQ against human ACE2 receptor, namely CYS344, TYR127, PRO346, MET360, LEU144, CYS361, ALA153, PHE274, TRP271, MET270, and LEU503 (Figure 4B). Although we have conducted the molecular docking studies of HCQ against the active site of the Human ACE2 receptor, however, to understand the exact mechanism, further screening needs to be done against other binding sites of human ACE2 and against the spike glycoprotein.

3.3 | MD simulation studies of LPN, RMD, and RTN against SARS-CoV-2 main protease

To understand the dynamic behavior and conformational flexibility of docked complexes, MD simulation of the three best drug complexes was performed for a time period of 100 ns. From the MD simulations, various thermodynamic properties were analyzed such as RMSD, the radius of gyration, root mean square fluctuation

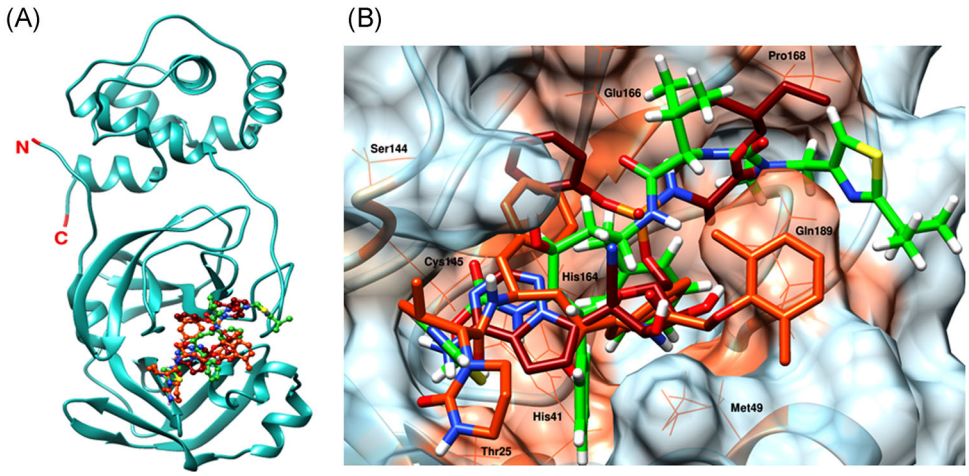

FIGURE 3 Superposition of best-docked complexes of drugs with SARS-Cov-2 Mpro. (A) Cartoon representation of overall docked complexes (B) Mode of drug binding at the active sites. SARS-CoV-2, severe acute respiratory syndrome coronavirus 2

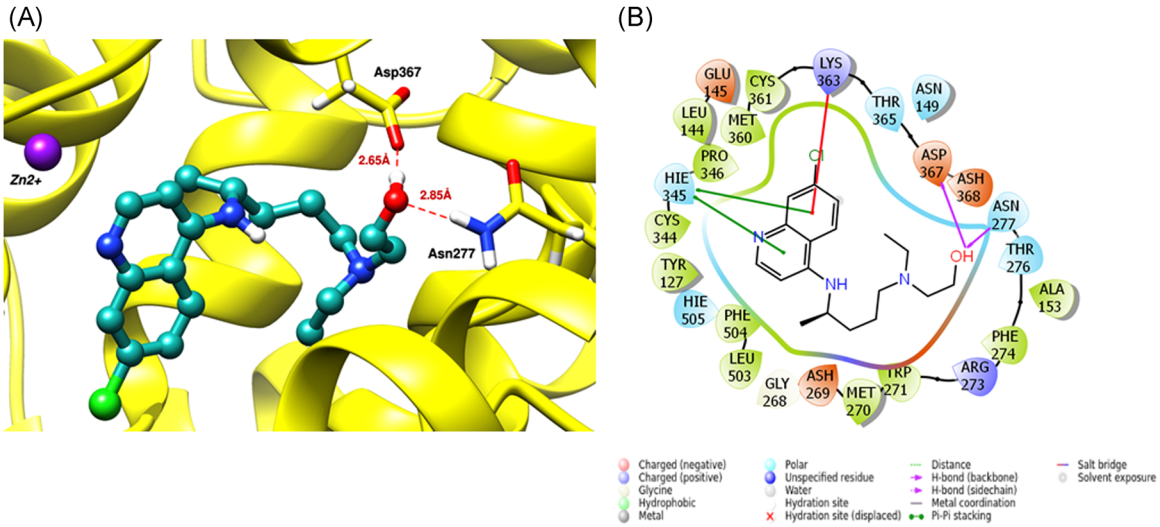

FIGURE 4 Key binding interaction profile of hydroxychloroquine (HCQ) docked with human ACE2 receptor (A) 3D chimera view (B) 2D maestro view. ACE2, angiotensin-converting enzyme II

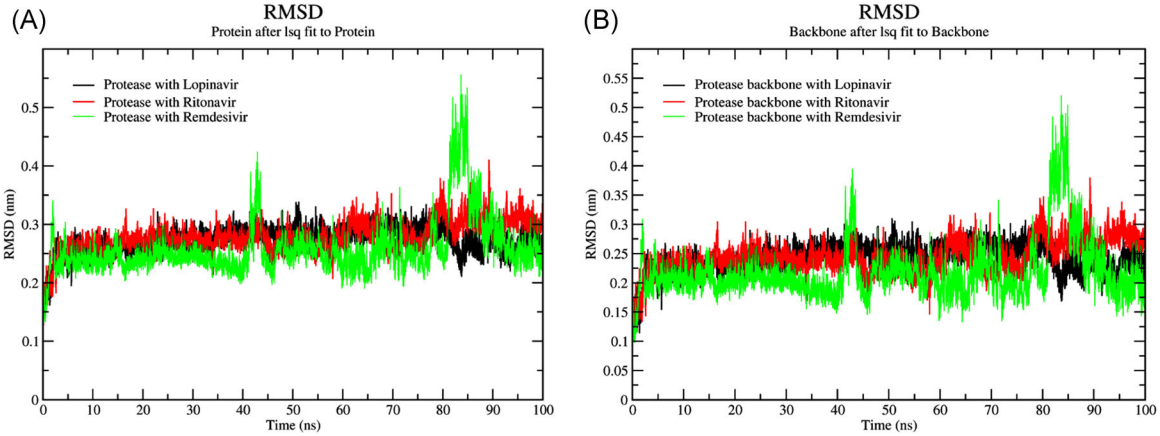

FIGURE 5 Root mean square deviations (RMSD) of best drugs Ritonavir (RTN), Remdesivir (RMD), and Lopinavir (LPN) during molecular dynamics (MD) simulation trajectory. (A) overall protein (B) backbone

(RMSF), ligand rmsf, and hydrogen bond contact analysis throughout the overall MD simulation.

From Figure 5A,B the same inferences can be derived. The first one was generated by fitting all atoms of the protein to all atoms of their own and the latter was generated by fitting the backbone atoms of the protein to the backbone atoms of their own for RMSD calculation. RMSD for the protease with RMD (green) is quite unstabilized when compared with the RMSD of the protease with LPN (black) and RTN (red).

Calculation of RMSD for the ligands was performed by excluding the hydrogen atoms of the ligands with respect to the protease backbones. By doing so, the overall rotation and translation of the protein are removed via fitting and the RMSD reported is how much the ligand position has varied relative to the protein, which is a good indicator of how well the binding pose was preserved during the simulation. Thus, it is observed that LPN (black) position from the binding pocket is comparatively varying when compared with the RTN (red) and RMD (green) (Figure 4S).

The radius of gyration of a protein is a measure of its compactness. If a protein is stably folded, it is likely to maintain a relatively steady value of Rg. If a protein unfolds, its Rg will change over time. In Figure 6, it is observed that the protease is not stably folded upon ligand binding. For instance, the protease with LPN (black) folds around 60 ns onwards as Rg decreases from 2.5 to 2.2 nm, whereas the proteases with RTN (red) and RMD (green) seems to be unfolded around 70 ns onwards as Rg suddenly increases from 2.175 to 2.25 nm (Figure 6).

The docked complexes' overall residual movements were calculated during the MD simulation, RMS Fluctuations for the amino acid residues of the protease from all three systems are in the same pattern. It is not very reflective due to ligand binding (Figure 7A). This trend in the RMSF plot for the protease indicates that the binding of three drugs to the protein was stable and had no major effect on the flexibility of the protein throughout the simulations. For RMS Fluctuations for the atoms of the ligands from all three systems, the atomic fluctuations of LPN (black) are comparatively less than that of the atomic fluctuations of RTN (red) and RMD (green). However, from the plot, it is observed that RTN is showing higher flexibility when compared with LPN and RMD (Figure 7B).

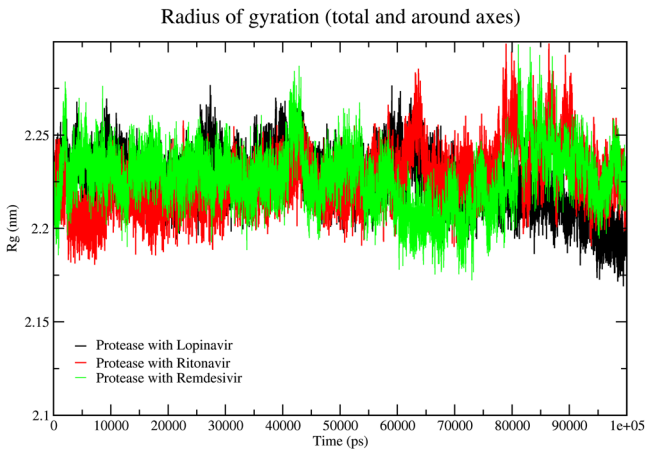

FIGURE 6 Radius of gyration for three best drugs Ritonavir (RTN), Remdesivir (RMD), and Lopinavir (LPN) during the molecular dynamics (MD) simulation

The minimum average distances between the ligand and protease are calculated. Close observation on the plot reflects that minimum distances between LPN (black) and protease as well as RTN (red) and protease are consistently maintained around 0.35 nm. However, the minimum distance between RMD and protease slightly increases from 0.3 to 0.35 nm (Figure 5S).

All three drugs show the same pattern of linear short-range Coulombic interactions. Average Coulombic short-range Protein–LPN (black) energy is −20.916 kJ/mol (red), Protein–RTN (green) energy is −32.1943 kJ/mol, and Protein–RMD energy is −31.2213 kJ/mol (Figure 8A). Lennard–Jones (LJ) interactions of LPN (black) and RTN (red) with the protease seemed to be promising as it is observed to be maintained at −225 kJ/mol and lowered below −250 kJ/mol from 60 to 87 ns. However, for RMD, LJ interactions are maintained at −200 kJ/mol and seemed to be lowered up to −225 kJ/mol at 60 ns only. Average Lennard–Jones short-range Protein–LPN (black) energy is −232.055 kJ/mol (red), Protein–RTN (green) energy is −227.69 kJ/mol, and Protein–RMD energy is −196.111 kJ/mol (Figure 8B).

Hydrogen bond contact analysis has been performed for three-drug docked complexes from the overall MD simulation trajectories. Results show that the RMD drug has more hydrogen bond contacts compared with the other two drugs throughout the MD simulation. All three-drug complexes are having a minimum of three hydrogen bond contacts from the simulated MD trajectories (Figure 6S).

3.4 | Conformational interaction of RTN, RMD, and LPN main protease binding sites from MD trajectories

To establish the stability of all three docked complexes and their binding sites interactions, a molecular visualization of the interaction snapshots (initial, 50, and 100 ns) over the simulation period was done. Recognition of key interactions that could have favored the binding affinity of docked compounds was observed.

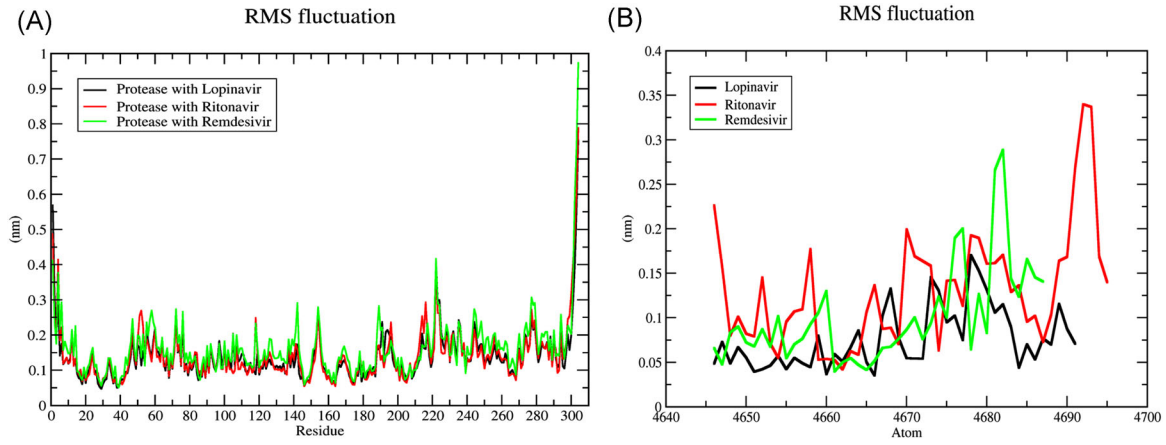

FIGURE 7 Root mean square (RMS) Fluctuation analysis from molecular dynamics (MD) trajectories. (A) Residual fluctuations of docked complexes of drugs (B) ligand RMS fluctuation of drugs

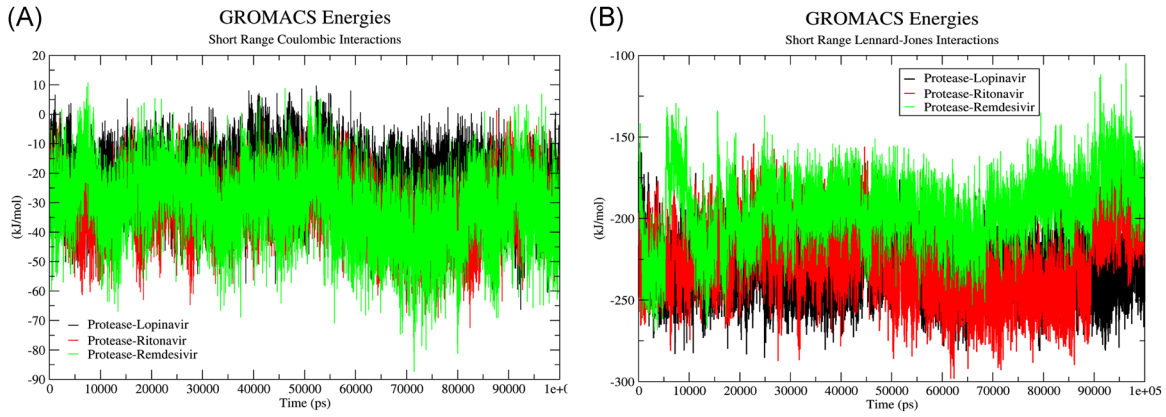

FIGURE 8 All three-drug complexes MD productions system energy. (A) Coulombic interactions from MD trajectories (B) Lennard–Jones interactions

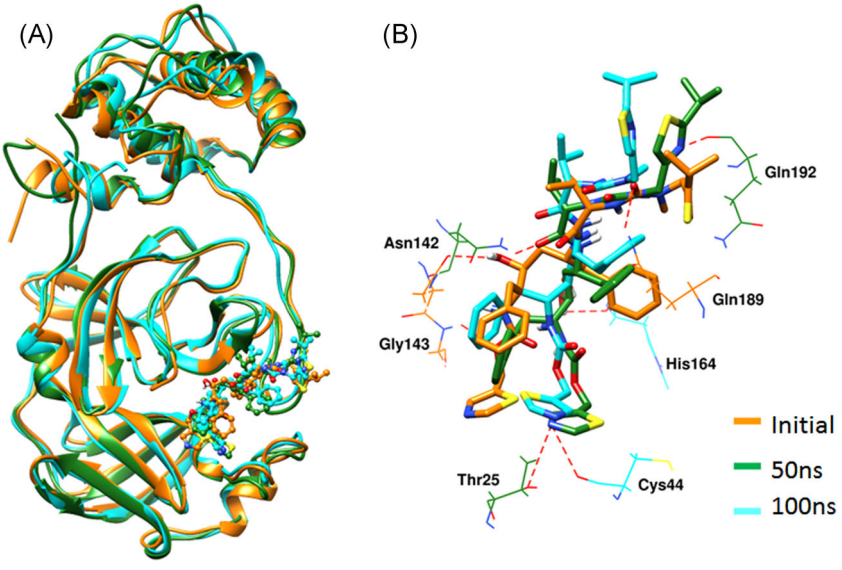

FIGURE 9 Molecular dynamics (MD) trajectories frame analysis of Ritonavir (RTN). (A) Superposition of three snapshot conformations. (B) Interaction profile of active sites

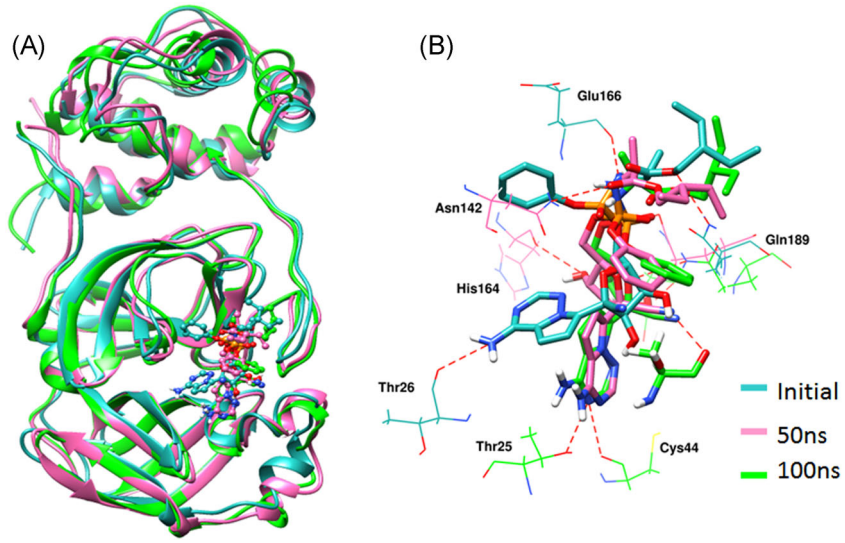

FIGURE 10 Molecular dynamics (MD) trajectories frame analysis of Remdesivir (RMD). (A) Superposition of three snapshot conformations. (B) Interaction profile of active sites

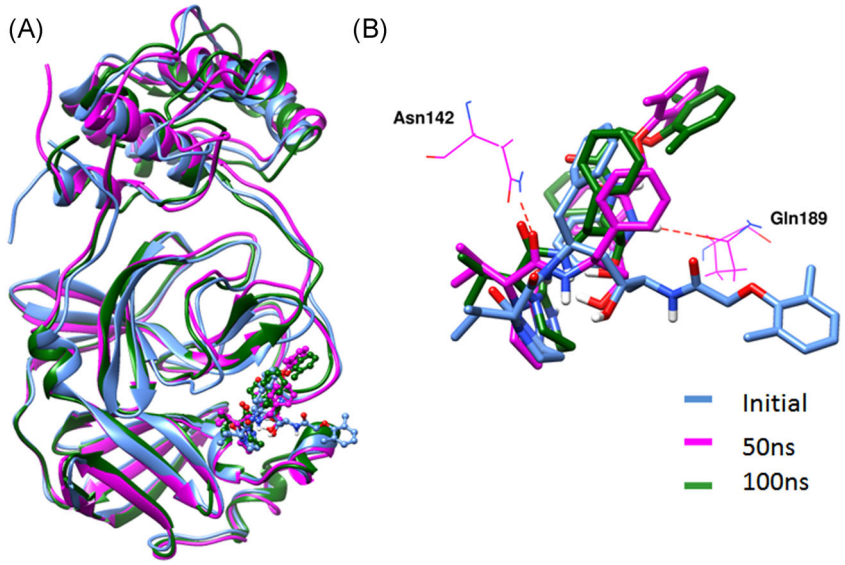

FIGURE 11 Molecular dynamics (MD) trajectories frame analysis of Lopinavir (LPN). (A) Superposition of three snapshot conformations. (B) Interaction profile of active sites

As shown in Figure 9A, all the three snapshot conformations of RTN drugs were superimposed, it depicts that all conformations are showing similar binding poses at the active sites of the targeted protein. Initial conformation, Gln189, and Gly143 found two hydrogen bond interactions with distances of 2.34 Å and 2.62 Å at the binding sites. At 50 ns, in addition, three strong hydrogen bond interactions were observed namely Gln192 (3.13 Å), Asn142 (2.94 Å), and Thr25 (3.12 Å). Towards the end of the MD simulation at 100 ns, which is important Cys44 (3.09 Å) and His164 (2.94 Å) showed hydrogen bond interaction with the RTN. Also, certain residues interacted consistently, across the overall MD simulation (Figure 9B).

Similarly, the RMD drug also shows a number of hydrogen bonds interactions at the active sites from the different snapshots during the MD simulation. Interactions with residues Gln189 (2.08 Å), Glu166 (3.05 Å), Asn142 (3.17 Å), His 164 (2.95 Å), Thr26 (3.14 Å), Thr25 (3.08 Å), and Cys44 (2.96 Å), reveals that RMD drug was more stable throughout the simulation and also all snapshot poses were superimposed and showed similar binding orientations at the active sites of protein Figure 10A,B.

In the case of LPN notably, Asn142 (2.02 Å) and Gln189 (1.96 Å) were found as hydrogen bond interaction with the respective drugs over the course of the simulation, as shown in the representative snapshots of 0, 50, and 100 ns. Figure 11A reveals that overall docked superposition protein backbone conformation slightly deviated. But initially, the drug does not show any conformational changes, at 50 and 100 ns MD simulation LPN drug entirely shifts the orientation of binding at the active sites (Figure 11B). One of the probable reasons for the change in orientation can be the structural flexibility of LPN as it is used as a combination drug with RTN.

TABLE 3 Binding free energy contributions of all the three drugs with Mpro (main protease)

MMPBSA					
	ΔE_{MM}		ΔG_{Sol}		
Protein–ligand complexes	ΔE_{VdW}	ΔE_{Elec}	ΔG_{PB}	ΔG_{SASA}	ΔG_{Bind}
Lopinavir–SARS-CoV-2 Mpro	−254.63 ± 14.99	−13.96 ± 6.24	121.31 ± 12.29	−24.37 ± 1.29	−171.65 ± 14.78
Ritonavir–SARS-CoV-2 Mpro	−252.02 ± 21.56	−16.45 ± 5.47	124.89 ± 26.08	−23.72 ± 1.63	−167.31 ± 30.59
Remdesivir–SARS-CoV-2 Mpro	−218.16 ± 19.55	−15.192 ± 8.16	112.73 ± 21.65	−19.58 ± 1.82	−140.20 ± 24.09

Interestingly, these three drugs exhibit common hydrogen bond interactions with important catalytic sites of Gln189 and Asn142 during the overall MD simulations.

3.5 | Binding free energy calculation (MM-PBSA)

During the MD simulation, the best drug compounds of RTN, LPN, and RMD docked complexes of Mpro were considered for the binding free energy calculation using the MM-PBSA approach. From the free energy calculation, it shows that van der Waals and electrostatic energetic terms mainly aids in the total binding energy (ΔG_{Total}). In Table 3, the best drugs docked complexes of main protease thermodynamic properties were tabulated such as van der Waals, electrostatic, polar, and nonpolar energy, solvent accessible surface area, and total energy. The LPN, RTN, and RMD compounds calculated Total binding energy (ΔG_{Total}) is −171.65, −167.31, and −140.20 kJ/mol, respectively. The above findings suggests that LPN showed better van der Waals and total binding energies ([−254.63 ± 14.99], [−171.65 ± 14.78]) compared with the other two drugs (RTN and RMD). The overall MD simulation, the thermodynamic contribution of three drugs such as polar, nonpolar solvation, electrostatics, and total binding energy were plotted in Figure 7S.

4 | CONCLUSIONS

Our in silico study revealed that the three drugs LPN, RTN, and RMD showed interaction with the active site residues of SARS-CoV-2 Mpro. RMSD of the protein-ligand complexes has maintained stability and complexes have remained stable during the simulations. The drug LPN changed orientation compared to RTN and RMD during MD simulation which is possible as RTN and LPN are used as a combination drug and not individually. Overall, among the FDA-approved drugs, in terms of total binding energy (ΔG_{Total}), LPN has a better binding affinity with the main protease compared to the other two drugs. We also observed from the docking studies that the prophylaxis mechanism of Hydroxychloroquine is possible by binding with the Human ACE2 receptor to prevent binding of the spike protein. Furthermore, studies are required to provide validation to the proposed mechanisms of action.

ACKNOWLEDGMENTS

The authors acknowledge Dr. Probodh Borah, Coordinator, Bioinformatics Infrastructure Facility, Head, Department of Animal Biotechnology, College of Veterinary Science, Assam Agricultural University, Khanapara, Guwahati, Assam, India for providing the facilities for carrying out molecular dynamics simulation studies. Author M.C. acknowledges the Institute Post-doctoral Fellowship of IIT Bombay, India. Author A.D. thank the Indian Council of Medical Research (ICMR), India for supporting his research by awarding a Senior Research Fellowship.

CONFLICT OF INTERESTS

The authors declare that there are no conflicts of interest.

AUTHOR CONTRIBUTIONS

Manisha Choudhury: Conceptualization, Methodology, Writing- Original draft preparation **Anantha Krishnan Dhanabalan**: Conceptualization, Methodology, Writing-Original draft preparation. **Nabajyoti Goswami**: Methodology, Validation.

DATA AVAILABILITY STATEMENT

The data that support the findings of this study are available from the corresponding author upon reasonable request.

ORCID

Manisha Choudhury https://orcid.org/0000-0002-6108-9040

Anantha K. Dhanabalan https://orcid.org/0000-0003-2774-853X

REFERENCES

1. Hui DS, Azhar I, Madani E, et al. The continuing 2019-nCoV epidemic threat of novel coronaviruses to global health: the latest 2019 novel coronavirus outbreak in Wuhan, China. *Int J Infect Dis*. 2020;91:264-266. doi:10.1016/j.ijid.2020.01.009

2. Wang M, Cao R, Zhang L, et al. Remdesivir and chloroquine effectively inhibit the recently emerged novel coronavirus (2019-nCoV) in vitro. *Cell Res*. 2020;30(3):269-271. doi:10.1038/s41422-020-0282-0
3. Hodos RA, Kidd BA, Shameer K, Readhead BP, Dudley JT. In silico methods for drug repurposing and pharmacology. *WIREs: Sys Biol Med*. 2016;8(3):186-210. doi:10.1002/wsbm.1337
4. Dobson J, Whitley RJ, Pocock S, Monto AS. Oseltamivir treatment for influenza in adults: a meta-analysis of randomised controlled trials. *Lancet*. 2015;385(9979):1729-1737. doi:10.1016/S0140-6736(14)62449-1
5. Wang Y, Lv Z, Chu Y. HIV protease inhibitors: a review of molecular selectivity and toxicity. *HIV AIDS (Auckl)*. 2015;7:95-104. doi:10.2147/HIV.S79956
6. Mercorelli B, Palù G, Loregian A. Drug repurposing for viral infectious diseases: how far are we? *Trends Microbiol*. 2018;26(10):865-876. doi:10.1016/j.tim.2018.04.004
7. Muralidharan N, Sakthivel R, Velmurugan D, Gromiha MM. Computational studies of drug repurposing and synergism of lopinavir, oseltamivir and ritonavir binding with SARS-CoV-2 protease against COVID-19. *J Biomol Struct Dyn*. 2020;39:1-6. doi:10.1080/07391102.2020.1752802
8. Bhardwaj VK, Singh R, Sharma J, Rajendran V, Purohit R, Kumar S. Identification of bioactive molecules from tea plant as SARS-CoV-2 main protease inhibitors. *J Biomol Struct Dyn*. 2020;1-10. doi:10.1080/07391102.2020.1766572
9. Bhardwaj VK, Singh R, Das P, Purohit R. Evaluation of acridinedione analogs as potential SARS-CoV-2 main protease inhibitors and their comparison with repurposed anti-viral drugs. *Comput Biol Med*. 2021;128(September 2020):104117. doi:10.1016/j.compbiomed.2020.104117
10. Bhardwaj VK, Singh R, Sharma J, Rajendran V, Purohit R, Kumar S. Bioactive molecules of tea as potential inhibitors for RNA-dependent RNA polymerase of SARS-CoV-2. *Front Med*. 2021;8(May):1-11. doi:10.3389/fmed.2021.684020
11. Singh R, Kumar V, Sharma J, Purohit R. In-silico evaluation of bioactive compounds from tea as potential SARS-CoV-2 non-structural protein 16 inhibitors. *J Tradit Complement Med*. Published online June 3, 2021.
12. Sharma J, Kumar Bhardwaj V, Singh R, Rajendran V, Purohit R, Kumar S. An in-silico evaluation of different bioactive molecules of tea for their inhibition potency against non structural protein-15 of SARS-CoV-2. *Food Chem*. 2021;346(December 2020):128933. doi:10.1016/j.foodchem.2020.128933
13. Singh R, Bhardwaj VK, Das P, Purohit R. A computational approach for rational discovery of inhibitors for non-structural protein 1 of SARS-CoV-2. *Comput Biol Med*. 2021;135:104555. doi:10.1016/j.compbiomed.2021.104555
14. Singh R, Bhardwaj VK, Sharma J, Kumar D, Purohit R. Identification of potential plant bioactive as SARS-CoV-2 Spike protein and human ACE2 fusion inhibitors. *Comput Biol Med*. 2021;136(July):104631. doi:10.1016/j.compbiomed.2021.104631
15. Li G, De Clercq E. Therapeutic options for the 2019 novel coronavirus (2019-nCoV). *Nat Rev Drug Discovery*. 2020;19(3):149-150. doi:10.1038/d41573-020-00016-0
16. Han DP, Penn-Nicholson A, Cho MW. Identification of critical determinants on ACE2 for SARS-CoV entry and development of a potent entry inhibitor. *Virology*. 2006;350(1):15-25. doi:10.1016/j.virol.2006.01.029
17. Savarino A, Di Trani L, Donatelli I, Cauda R, Cassone A. New insights into the antiviral effects of chloroquine. *Lancet Infect Dis*. 2006;6(2):67-69. doi:10.1016/S1473-3099(06)70361-9
18. Gautret P, Lagier J-C, Parola P, et al. Hydroxychloroquine and azithromycin as a treatment of COVID-19: results of an open-label non-randomized clinical trial. *Int J Antimicro Ag*. 2020;56:105949. doi:10.1016/j.ijantimicag.2020.105949
19. Ip A, Ahn J, Zhou Y, et al. Hydroxychloroquine in the treatment of outpatients with mildly symptomatic COVID-19: a multi-center observational study. *BMC Infect Dis*. 2021;21(1):72. doi:10.1186/s12879-021-05773-w
20. Zhao Q, Weber E, Yang H. Recent developments on coronavirus main protease/3C like protease inhibitors. *Recent Pat Anti-Infect Drug Disc*. 2013;8(2):150-156. doi:10.2174/1574891X113089990017
21. Anand K. Structure of coronavirus main proteinase reveals combination of a chymotrypsin fold with an extra alpha-helical domain. *EMBO J*. 2002;21(13):3213-3224. doi:10.1093/emboj/cdf327
22. Shi J, Wei Z, Song J. Dissection study on the severe acute respiratory syndrome 3C-like protease reveals the critical role of the extra domain in dimerization of the enzyme. *J Biol Chem*. 2004;279(23):24765-24773. doi:10.1074/jbc.M311744200
23. Schrödinger Release 2014-2. LigPrep, Schrödinger, LLC, New York, NY. 2014.
24. Shelley JC, Cholleti A, Frye LL, Greenwood JR, Timlin MR, Uchimaya M. Epik: a software program for pK a prediction and protonation state generation for drug-like molecules. *J Comput Aided Mol Des*. 2007;21(12):681-691. doi:10.1007/s10822-007-9133-z
25. Shivakumar D, Williams J, Wu Y, Damm W, Shelley J, Sherman W. Prediction of absolute solvation free energies using molecular dynamics free energy perturbation and the opls force field. *J Chem Theory Comput*. 2010;6(5):1509-1519. doi:10.1021/ct900587b
26. Schrödinger Release 2014-2. Protein Preparation Wizard; Epik, Schrödinger, LLC, New York, NY, 2014; Impact, Schrödinger, LLC, New York, NY, 2014; Prime, Schrödinger, LLC, New York, NY. 2014.
27. Jacobson MP, Friesner RA, Xiang Z, Honig B. On the role of the crystal environment in determining protein side-chain conformations. *J Mol Biol*. 2002;320(3):597-608. doi:10.1016/S0022-2836(02)00470-9
28. Schrödinger Glide, version 6.0. Schrödinger, LLC; New York, NY. 2014.
29. Friesner RA, Murphy RB, Repasky MP, et al. Extra precision glide: docking and scoring incorporating a model of hydrophobic enclosure for protein−ligand complexes. *J Med Chem*. 2006;49(21):6177-6196. doi:10.1021/jm051256o
30. Genheden S, Ryde U. The MM/PBSA and MM/GBSA methods to estimate ligand-binding affinities. *Expert Opin Drug Discovery*. 2015;10(5):449-461. doi:10.1517/17460441.2015.1032936
31. Hess B, Kutzner C, van der Spoel D, Lindahl E. GROMACS 4: algorithms for highly efficient, load-balanced, and scalable molecular simulation. *J Chem Theory Comput*. 2008;4(3):435-447. doi:10.1021/ct700301q

32. Lindahl E, Hess B, van der Spoel D. GROMACS 3.0: a package for molecular simulation and trajectory analysis. *J Mol Model*. 2001;7(8):306-317. doi:10.1007/s008940100045
33. Lindorff-Larsen K, Piana S, Palmo K, et al. Improved side-chain torsion potentials for the Amber ff99SB protein force field. *Proteins*. 2010;78:1950-1958. doi:10.1002/prot.22711
34. Páll S, Abraham MJ, Kutzner C, Hess B, Lindahl E. Tackling exascale software challenges in molecular dynamics simulations with GROMACS. *Proc EASC*. 2015:3-27. doi:10.1007/978-3-319-15976-8_1
35. Pronk S, Páll S, Schulz R, et al. GROMACS 4.5: a high-throughput and highly parallel open source molecular simulation toolkit. *Bioinformatics*. 2013;29(7):845-854. doi:10.1093/bioinformatics/btt055
36. Berendsen HJC, van der Spoel D, van Drunen R. GROMACS: a message-passing parallel molecular dynamics implementation. *Comput Phys Commun*. 1995;91(1–3):43-56. doi:10.1016/0010-4655(95)00042-E
37. Van Der Spoel D, Lindahl E, Hess B, Groenhof G, Mark AE, Berendsen HJC. GROMACS: fast, flexible, and free. *J Comput Chem*. 2005;26(16):1701-1718. doi:10.1002/jcc.20291
38. Sousa da Silva AW, Vranken WF. ACPYPE - AnteChamber PYthon Parser interfacE. *BMC Res Notes*. 2012;5(1):367. doi:10.1186/1756-0500-5-367
39. Baker NA, Sept D, Joseph S, Holst MJ, McCammon JA. Electrostatics of nanosystems: application to microtubules and the ribosome. *Proc Natl Acad Sci USA*. 2001;98(18):10037-10041. doi:10.1073/pnas.181342398
40. Kumari R, Kumar R, Lynn A. g_mmpbsa: a GROMACS tool for high-throughput MM-PBSA calculations. *J Chem Inf Model*. 2014;54(7):1951-1962. doi:10.1021/ci500020m
41. Homeyer N, Gohlke H. Free energy calculations by the molecular mechanics poisson−Boltzmann surface area method. *Mol Inf*. 2012;31(2):114-122. doi:10.1002/minf.201100135
42. Ullrich S, Nitsche C. The SARS-CoV-2 main protease as drug target. *Bioorg Med Chem Lett*. 2020;30(17):127377. doi:10.1016/j.bmcl.2020.127377
43. Sacco MD, Ma C, Lagarias P, et al. Structure and inhibition of the SARS-CoV-2 main protease reveal strategy for developing dual inhibitors against M pro and cathepsin L. *Sci Adv*. 2020;6(50):eabe0751. doi:10.1126/sciadv.abe0751
44. Cui W, Yang K, Yang H. Recent progress in the drug development targeting SARS-CoV-2 main protease as treatment for COVID-19. *Front Mol Biosci*. 2020;7:7. doi:10.3389/fmolb.2020.616341

SUPPORTING INFORMATION

Additional supporting information may be found in the online version of the article at the publisher's website.

How to cite this article: Choudhury M, Dhanabalan AK, Goswami N. Understanding the binding mechanism for potential inhibition of SARS-CoV-2 Mpro and exploring the modes of ACE2 inhibition by hydroxychloroquine. *J Cell Biochem*. 2022;123:347-358. doi:10.1002/jcb.30174